2009 American Control Conference
Hyatt Regency Riverfront, St. Louis, MO, USA
June 10-12, 2009

Servo-Hydraulic Actuator Control for Real-Time Hybrid Simulation

Cheng Chen and James M. Ricles

Abstract— **Real-time hybrid simulation combines experimental testing with numerical simulation, enabling the complete structural system to be considered in an experiment. The method presents an economical and effective technique to physically evaluate the behavior of rate-dependent seismic devices and to validate performance-based design procedures. Accurate servo-hydraulic actuator control is necessary for a successful real-time hybrid simulation. Inherent servo-hydraulic actuator dynamics can lead to actuator delay that results in a desynchronization between the measured restoring force(s) and the integration algorithm, leading to inaccurate results and possible instability in the simulation. This paper presents an adaptive compensation scheme to achieve accurate actuator control in real-time hybrid simulation. Experimental evaluation of the proposed adaptive scheme is conducted for a single-degree-of-freedom moment resisting frame with an elastomeric damper. The performance of the adaptive compensation scheme is compared with other compensation methods. It is shown that the adaptive compensation scheme is able to achieve accurate actuator control in real-time hybrid simulation.**

I. Introduction

Real-time hybrid simulation, also known as real-time substructure testing, is a viable and economic technique for investigating the dynamic response of structural systems. It divides a structural system into experimental substructure(s) and analytical substructure(s), and thus enables the complete structural system to be considered during the test. A number of rate-dependent devices have been developed to enhance the seismic performance of structural systems during earthquakes [1], of which the restoring force is dependent on the rate of the deformation. The development of performance-based design procedures for structures with these devices requires that the device's behavior be well understood, the performance of the structural system with the devices be evaluated, and the design procedure be verified. These requirements can be economically satisfied by performing real-time hybrid simulation of structural systems with these devices to acquire reliable experiment data.

During a real-time hybrid simulation, the displacement response (also called command displacements) of the structural system is calculated using an integration algorithm and the restoring forces from substructures that are developed under imposed command displacements. The experimental and analytical substructures, the integration algorithm, and the servo-hydraulic actuator(s) combine together to form the real-time hybrid simulation system. Unlike conventional hybrid simulation, real-time hybrid simulation requires that the actuator(s) accurately impose the command displacement(s) onto the experimental substructure(s) at a real-time scale. Accurate actuator control is therefore necessary for a successful real-time hybrid simulation. However, due to inherent servo-hydraulic dynamics, the actuator has an inevitable delay in response to the command displacement. This time delay is usually referred to as actuator delay.

The effect of actuator delay on real-time hybrid simulation has attracted the attention of numerous researchers [2]-[3]. Wallace *et al.* [4] performed stability analysis of real-time hybrid simulation using a delay differential equation. Chen and Ricles [5] introduced discrete control theory to include explicit integration algorithms in the stability analysis and investigated the effect of actuator delay on the entire real-time hybrid simulation. These studies show that actuator delay is equivalent to negative damping and can destabilize a real-time hybrid simulation if not compensated properly.

Actuator delay compensation is often used in real-time hybrid simulation to achieve accurate actuator control. Horiuchi *et al.* [3], [6] proposed two compensation schemes based on polynomial extrapolation and a linear acceleration assumption, respectively. Compensation methods originating from control engineering practice have also been investigated such as derivative feedforward [7]. Chen [8] proposed a simplified discrete transfer function model for the servo-hydraulic actuator and applied the inverse of the model for actuator delay compensator. These compensation methods are developed for a constant actuator delay. Applying these compensation methods in real-time hybrid simulation require an accurate estimate of actuator delay. Estimating an accurate delay however can be difficult in actual practice. Moreover the actuator delay might vary during the simulation due to the nonlinearity in the experimental substructure. Based on the inverse compensation method, Chen and Ricles [9] proposed a dual compensation method using the actuator control error to improve the performance of inverse compensation method with an inaccurate estimate of actuator delay. Compensation methods based on adaptive control theory also have been proposed. Darby *et al.* [10] proposed an online procedure to estimate and compensate actuator delay during a real-time hybrid simulation. Bonnet *et al.* [11] applied model reference adaptive minimal control synthesis (MCS) to real-time hybrid simulation.

Cheng Chen is with the ATLSS Engineering Research Center, Lehigh University, Bethlehem, PA 18015 USA (corresponding author: 610-758-5524; fax: 610-758-5333; e-mail: chc4@ Lehigh.edu).

James M. Ricles is with the ATLSS Engineering Research Center, Lehigh University, Bethlehem, PA 18015 USA (e-mail: jmr5@lehigh.edu).

978-1-4244-4524-0/09/$25.00 ©2009 AACC

In this paper, an adaptive inverse compensation method is proposed to achieve accurate actuator control in real-time hybrid simulation. An adaptive control law is developed to adapt the compensation parameter to minimize the effect of an unknown and time varying actuator delay in a real-time hybrid simulation. The proposed adaptive method is shown to require minimal information about the experiment. It is experimentally evaluated by real-time hybrid simulations of a single-degree-of-freedom (SDOF) moment resisting frame (MRF) with an elastomeric damper. The performance of the proposed adaptive inverse compensation method is also compared with the inverse compensation and the dual compensation methods. It is shown that actuator control is significantly improved using the adaptive inverse compensation, and can thereby enable a reliable real-time hybrid simulation.

II. INVERSE COMPENSATION

For the real-time hybrid simulation of a SDOF structural model as shown in Fig. 1, the equation of motion can be written as

$$m \cdot \ddot{x}(t) + c \cdot \dot{x}(t) + r_a(t) + r_e(t) = F(t) \qquad (1a)$$

where m and c are the mass and the inherent viscous damping of the structure, respectively; $\dot{x}(t)$ and $\ddot{x}(t)$ are the velocity and acceleration response, respectively; $F(t)$ is the predefined external excitation force; and $r_a(t)$ and $r_e(t)$ are the restoring forces of the analytical and physical substructures, respectively. The combination of $r_a(t)$ and $r_e(t)$ provides the total resistance of the SDOF structure to the dynamic load. For linear elastic substructures, the restoring forces can be written as $r_a(t) = k_a \cdot x(t)$ and $r_e(t) = k_e \cdot x(t)$, where k_e and k_a are the linear elastic stiffness of the experimental and analytical substructures, respectively, and $x(t)$ is the displacement response of the SDOF structure.

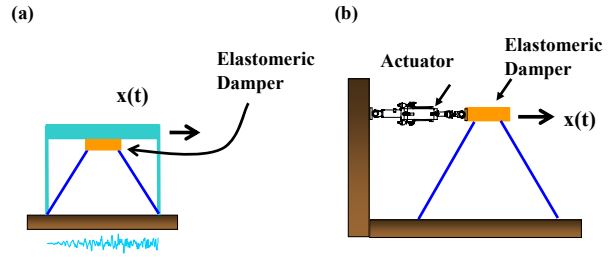

Figure 1 (a) SDOF with elastomeric damper, (b) experimental substructure

An integration algorithm is utilized in a real-time hybrid simulation to numerically solve the temporally discretized form of Eq. (1a), which can be expressed as

$$m \cdot \ddot{x}_{i+1} + c \cdot \dot{x}_{i+1} + r_{a,i+1} + r_{e,i+1} = F_{i+1} \qquad (1b)$$

where $\ddot{x}_{i+1}$, $\dot{x}_{i+1}$, F_{i+1} are the acceleration, velocity, and the excitation force at time step i+1, respectively; and $r_{e,i+1}$ and $r_{a,i+1}$ are restoring forces of the experimental and analytical substructures at time step i+1. The displacement response determined by the integration algorithm, x_{i+1}, is then transferred to the command displacements for the physical and analytical substructures. For the SDOF structure discussed in this paper (as shown in Fig. 1), the command displacements for the physical and analytical substructures at time step i+1 are the same as x_{i+1} of the SDOF structure at time step i+1.

The command displacement x_{i+1} for the experimental substructure (referred to as the actuator command displacement) is usually imposed by a servo-hydraulic actuator in a real-time hybrid simulation. To ensure a smooth actuator response and reduce possible actuator displacement overshoot, a ramp generator is used to interpolate the command displacement x_{i+1} over the integration time step Δt. Δt is typically an integer multiple of the servo-controller sampling time δt. For a linear ramp generator, the actuator command displacement sent to the servo-controller is interpolated as

$$d_{i+1}^{c(j)} = \frac{j}{n} \cdot (x_{i+1} - x_i) + x_i \qquad (2)$$

In Eq. (2) j is the index for the interpolation substep of the ramp generator in one single time step. j ranges from 1 to n, where n is the integer ratio of $\Delta t/\delta t$. In Eq. (2) $d_{i+1}^{c(j)}$ is the command displacement for the actuator at the j^{th} substep of the $(i+1)^{th}$ time step. Eq. (2) can be modified when other forms of ramp generators are used, (e.g., a quadratic ramp generator).

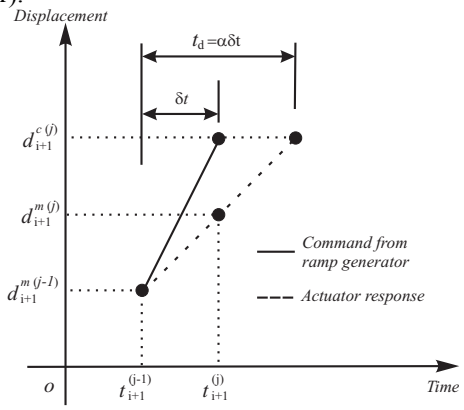

Figure 2 Actuator response with a time delay

Due to actuator delay, the servo-hydraulic actuator will achieve a measured displacement $d_{i+1}^{m(j)}$ instead of the command displacement $d_{i+1}^{c(j)}$. For the time interval of δt, which is typically 1/1024 *sec*. for state-of-art digital servo-controllers, the actuator response can be idealized as a linear response, as shown in Fig. 2. The duration for the actuator to achieve the command displacement $d_{i+1}^{c(j)}$ is t_d, where t_d is equal to $\alpha\delta t$. The parameter α is greater than 1.0 when a time delay exists in the actuator response. Assuming that the actuator achieves the displacement $d_{i+1}^{m(j-1)}$ at the end of the $(j-1)^{th}$ substep during the $(i+1)^{th}$ integration time step, and using the linear actuator response shown in Fig. 2, the measured displacement response $d_{i+1}^{m(j)}$ at the end of the j^{th} substep of the $(i+1)^{th}$ time step can be expressed as

$$d_{i+1}^{m(j)} = d_{i+1}^{m(j-1)} + \frac{1}{\alpha} \cdot (d_{i+1}^{c(j)} - d_{i+1}^{m(j-1)}) \qquad (3)$$

Applying the discrete z-transform [12] to Eq. (3) leads to a discrete transfer function $G_d(z)$ relating the measured actuator response $d_{i+1}^{m(j)}$ to the command displacement $d_{i+1}^{c(j)}$, where

$$G_d(z) = \frac{X^m(z)}{X^c(z)} = \frac{z}{\alpha \cdot z - (\alpha - 1)} \tag{4}$$

In Eq. (4) z is the complex variable in the discrete z-domain, and $X^m(z)$ and $X^c(z)$ are the discrete z-transforms of $d_{i+1}^{m(j)}$ and $d_{i+1}^{c(j)}$, respectively.

Chen [8] proposed to use the inverse dynamics of Eq. (4) for actuator delay compensation to achieve accurate actuator control in a real-time hybrid simulation, whereby the discrete transfer function for the resulting inverse compensation method can be written as

$$G_c(z) = \frac{X_d^p(z)}{X_d^c(z)} = \frac{\alpha \cdot z - (\alpha - 1)}{z} \tag{5}$$

where $X_d^p(z)$ is the discrete z-transform of the predicted displacement $x_{i+1}^{p(j)}$ to be sent to the servo controller for the j^{th} substep at time step i+1.

III. ADAPTIVE INVERSE COMPENSATION

Chen *et al.* [13] applied the inverse compensation to real-time hybrid simulation of structures with an elastomeric damper. Good actuator tracking was observed when an accurate value of α was used. However, an accurate estimate of actuator delay, i.e., the value of α, may not be available for a real-time hybrid simulation. Moreover, the actuator delay may vary due to the nonlinearity in the experimental substructure. Estimated actuator delay based on previous experience therefore has to be used, which may not be accurate and consequently result in over- or under-compensation of actuator delay in a real-time hybrid simulation. To minimize the effect of an inaccurately estimated or time varying actuator delay for a real-time hybrid simulation, an adaptive compensation method is proposed in this paper based on the inverse compensation method in Eq. (5). The adaptive compensation method is formulated as

$$G_c(z) = \frac{X^p(z)}{X^c(z)} = \frac{(\alpha_{es} + \Delta\alpha) \cdot z - (\alpha_{es} + \Delta\alpha - 1)}{z} \tag{6}$$

where $\Delta\alpha$ is an evolutionary variable during the real-time hybrid simulation that has an initial value of zero. The adaptive control law for $\Delta\alpha$ is based on a tracking indicator (TI) and is defined as

$$\Delta\alpha(t) = k_p \cdot TI(t) + k_I \cdot \int_0^t TI(\tau) d\tau \tag{7}$$

where k_p and k_I are proportional and integrative gains, respectively. The TI is based on the enclosed area of the hysteresis in the synchronized subspace plot shown in Fig. 3, where the actuator command displacement d^c is plotted against the actuator measured response d^m. The calculation of TI at each time step can be formulated as [14]

$$TI_{i+1}^{(j)} = 0.5\left(A_{i+1}^{(j)} - TA_{i+1}^{(j)}\right) \tag{8}$$

In Eq. (8), $A_{i+1}^{(j)}$ and $TA_{i+1}^{(j)}$ are the enclosed and complementary enclosed areas for the j^{th} substep at time step i+1, respectively, and are defined as

$$A_{i+1}^{(j)} = A_{i+1}^{(j-1)} + 0.5\left(d_{i+1}^{c(j)} + d_{i+1}^{c(j-1)}\right)\left(d_{i+1}^{m(j)} - d_{i+1}^{m(j-1)}\right) \tag{9a}$$

$$TA_{i+1}^{(j)} = TA_{i+1}^{(j-1)} + 0.5\left(d_{i+1}^{m(j)} + d_{i+1}^{m(j-1)}\right)\left(d_{i+1}^{c(j)} - d_{i+1}^{c(j-1)}\right) \tag{9b}$$

At the beginning of the test, A and TA have initial values of zero. The calculation of A and TA continues for every substep of each time step until the end of the real-time hybrid simulation. Mercan [14] showed that a positive rate of change of TI corresponds to an actuator response lagging behind the command displacement, where energy is introduced into the real-time hybrid simulation; while a negative rate of change indicates a leading actuator response, where artificial damping is added into the real-time simulation. A zero rate of change implies no actuator control error, i.e., the actuator measured and command displacements are equal to each other.

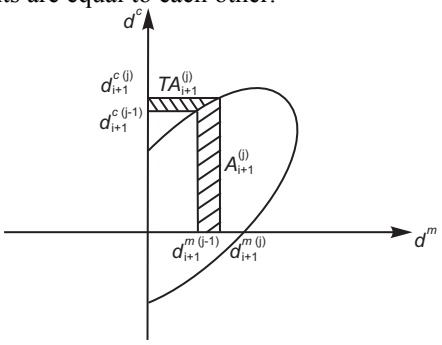

Figure 3 Definition of tracking indicator [14]

Eq. (7) gives the adaptation of $\Delta\alpha$ in continuous form. For practical application, Eq. (7) needs to be implemented in a discrete form, which can be formulated as

$$\Delta\alpha(z) = k_p \cdot TI(z) + k_I \cdot \frac{\delta t}{z - 1} \cdot TI(z) \tag{10}$$

where $\Delta\alpha(z)$ and $TI(z)$ are discrete z-transforms of $\Delta\alpha$ and the TI, respectively. It can be observed that the adaptation of $\Delta\alpha$ in Eqs. (7) and (10) depends on the values of k_p and k_I. Generally, a larger value of k_p results in a faster response and a larger oscillation in the actuator displacement, while increasing the integrative gain k_I reduces the oscillation and leads to smaller steady state error. In this paper, the integrative gain k_I is selected to be one tenth of the proportional gain k_p based on the numerical simulation to achieve a fast adaptation with a small overshoot. Fig. 4 shows the block diagram for the adaptive inverse compensation method for real-time hybrid simulation.

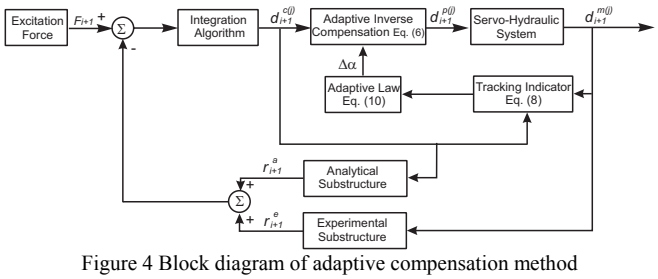

Figure 4 Block diagram of adaptive compensation method

IV. EXPERIMENTAL EVALUATION

To evaluate the performance of the proposed adaptive compensation method for actuator control for real-time hybrid simulation, real-time hybrid simulations are conducted for a SDOF MRF with an elastomeric damper. The explicit CR integration algorithm is used [15], of which the variations of displacement and velocity over the time step are defined as

$$\dot{x}_{i+1} = \dot{x}_i + \Delta t \cdot \alpha_1 \cdot \ddot{x}_i \quad (11a)$$

$$x_{i+1} = x_i + \Delta t \cdot \dot{x}_i + \Delta t^2 \cdot \alpha_2 \cdot \ddot{x}_i \quad (11b)$$

To incorporate the rate-dependent properties of the elastomeric damper in the real-time hybrid simulation, the integration parameters α_1 and α_2 are defined as

$$\alpha_1 = \alpha_2 = \frac{4m}{4 \cdot m + 2 \cdot \Delta t \cdot (c + c_{eq}) + \Delta t^2 \cdot (k_{eq} + k_a)} \quad (12)$$

where c_{eq} and k_{eq} are the equivalent damping and equivalent stiffness of the elastomeric damper, respectively. The values of k_{eq} and c_{eq} were determined from damper characterization tests and are equal to 7.6kN/mm and 0.64kN-sec/mm, respectively. The CR integration algorithm in Eqs. (11a) and (11b) can be observed to be explicit for both displacement and velocity. Using the discrete transfer function approach, Chen and Ricles [15] showed that the CR integration algorithm is unconditionally stable for a linear elastic structure.

The SDOF MRF in Fig. 1 without the elastomeric damper has a mass of 503.4 metric tons, an elastic natural frequency of 0.77 Hz, and an inherent viscous damping ratio ζ of 0.02. The SDOF MRF is taken as the analytical substructure and modeled using the Bouc-Wen model [16], whereby the restoring force of the MRF is expressed as

$$r_a(t) = \eta \cdot k_a \cdot x_a\ (t) + (1-\eta) \cdot k_a \cdot x_{a,y} \cdot z(t) \quad (13)$$

In Eq. (13) $x_{a,y}$ is the yield displacement of the SDOF MRF; k_a is the linear elastic stiffness of the SDOF MRF; η is the ratio of the post- to pre-yield stiffness of the SDOF MRF; $x_a(t)$ is the displacement applied to the MRF by the integration algorithm; and $z(t)$ is a evolutionary parameter of the Bouc-Wen model governed by the following differential equation:

$$x_{a,y} \cdot \dot{z}(t) + \gamma \left|\dot{x}_a(t)\right| \cdot z(t) \cdot \left|z(t)\right|^{q-1} + \beta \cdot \dot{x}_a(t) \cdot \left|z(t)\right|^q - \dot{x}_a(t) = 0 \quad (14)$$

The dimensionless parameters γ, β and q in Eq. (14) control the shape of the hysteretic loop of the analytical substructure [16]. The properties of the Bouc-Wen model for the analytical substructure are given in Table 1.

TABLE 1 VALUES FOR PARAMETERS OF THE BOUC-WEN MODEL FOR THE ANALYTICAL SUBSTRUCTURE

Parameter	k_a (KN/mm)	η	$x_{a,y}$ (mm)	β	γ	q
Value	11.76	0.01	10	0.55	0.45	2

The time step Δt for the real-time hybrid simulation in the experimental validation is selected as 10/1024 *sec.* and is ten times the servo-controller sampling time δt. The N196E component of the 1994 Northridge earthquake recorded at Canoga Park is selected as the ground motion and is scaled to have a maximum acceleration of 0.322 m/s^2 to ensure a maximum displacement response of less than 40 mm not to damage the elastomeric damper.

Fig. 5 shows the experimental setup, which consists of the experimental substructure (elastomeric damper), the servo-hydraulic actuator with a support and roller bearings, and two reaction frames. The elastomeric damper has the characteristics of an elastomeric material at small deformation amplitudes, with friction dominating the behavior at larger amplitudes. The servo-controller for the actuator used in real-time hybrid simulations consisted of a digital PID controller with the proportional gain of 20, integral time constant of 5.0 resulting in an integral gain of 4.0, differential gain of 0 and a roll-off frequency of 39.8 Hz.

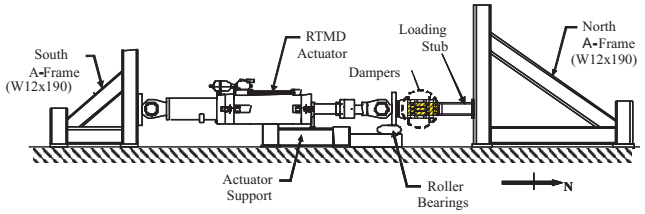

Figure 5 Experimental setup for real-time hybrid simulation

To systematically evaluate the performance of the proposed adaptive compensation method, different values are used for α_{es} in Eq. (7), including α_{es} equal to 15, 29 and 45. From real-time tests using a predefined sinusoidal displacement, a value of α_{es}=29 is selected to represent an accurate estimation for actuator delay. Values of α_{es}=15 and α_{es}=45 correspond to poor estimates of actuator delay and represent an error in the estimated actuator delay of about ±50% when compared with α_{es}=29. A value of k=3.0 is selected for the simulations with dual compensation method [9]. For the simulations with adaptive compensation method, the proportional gain k_p is selected to be 0.4 based on numerical simulations. The proportional gain k_I is therefore 0.04. For the purpose of comparison, real-time hybrid simulations with inverse and dual compensation are also conducted for the same SDOF structure with the elastomeric damper. Figs. 6 through 8 present the real-time hybrid simulation results using the three compensation methods with the value for the estimated actuator delay of α_{es} equal to 29, 15 and 45, respectively.

Fig. 6(a) shows the comparison of the command displacement and the measured actuator displacement for the real-time hybrid simulation with adaptive compensation method using α_{es}=29. Good tracking can be observed. The displacement history has maximum and minimum values of around 34.2 mm and -10.6 mm, respectively. Yielding of the analytical substructure occurred, beginning at around 15 *sec.* resulting in a residual drift of 21.4 mm at the end of the simulation. Figs. 6(b), (c), and (d) show a comparison of the real-time hybrid simulation results using the inverse, dual, and adaptive compensation methods where they are labeled as *inverse*, *dual k=3.0* and *adaptive* k_p*=0.4*, respectively. The difference between the command displacements and measured actuator displacements (referred to as *control*

error) is presented in Fig. 6(b). A maximum magnitude of 0.30 mm can be observed for the actuator control error, indicating an almost perfect actuator tracking during the simulation for all three simulations. Fig. 6(c) shows the TI values for the real-time hybrid simulations. The simulations with adaptive compensation and dual compensation are observed to have a minimum value of -4, while the simulation using the inverse compensation method is observed to have a larger magnitude for the TI. These results show an improved actuator tracking for the real-time hybrid simulations that use either the dual or adaptive compensation. For the case with inverse compensation, the varying slope of the tracking indicator implies a variable actuator delay in the real-time hybrid simulation. The hybrid simulation energy monitor (HSEM) for the real-time hybrid simulation results is also used to evaluate the simulation results and is presented in Fig. 6(d) [17]. The HSEM is observed to be less than 1% of the input energy for all three real-time hybrid simulations, where the HSEM of the simulation with adaptive compensation has the smallest value.

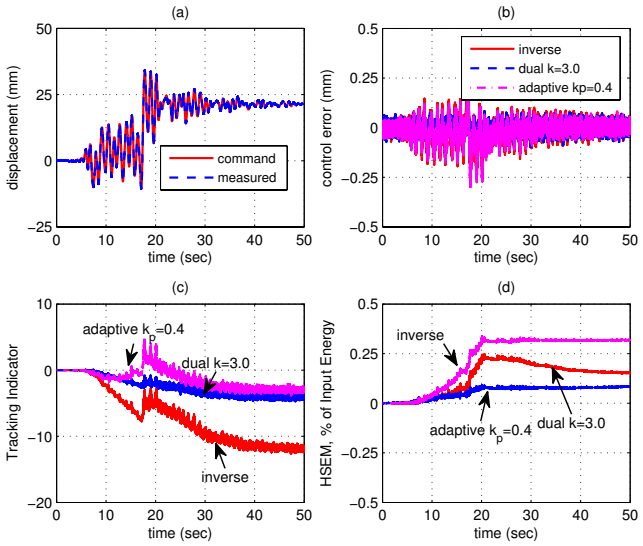

Figure 6 Real-time hybrid simulation results using compensation methods with α_{es}=29: (a) comparison of measured actuator response; (b) control error; (c) tracking indicator; (d) HSEM.

Figs. 7 and 8 present the real-time hybrid simulation results with α_{es}=15 and α_{es}=45, respectively. The comparisons of the command displacements with the measured actuator displacements are presented in Figs. 7(a) and 8(a) for the simulations with adaptive compensation method. The control errors between the command displacements and the measured actuator displacements for the simulations are shown in Figs. 7(b) and 8(b). It can be observed that due to the poor estimates of actuator delay, the control errors in Figs. 7(b) and 8(b) are larger than those in Fig. 6(b). However, in both Figs. 7(b) and 8(b), the real-time hybrid simulation with adaptive compensation have the smallest magnitude of less than 0.25 mm for the control error, which is smaller than that in the simulations with inverse compensation (where the maximum control error is 1.5 mm) and dual compensation (where the control error is 0.5 mm).

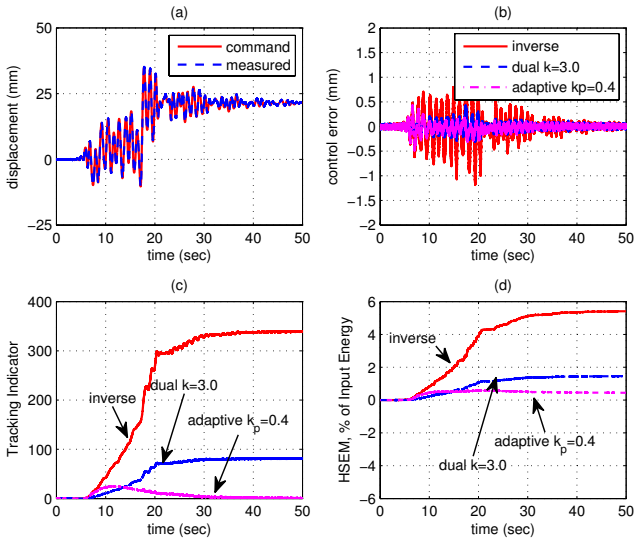

Figure 7 Real-time hybrid simulation results using compensation methods with α_{es}=15: (a) comparison of measured actuator response; (b) control error; (c) tracking indicator; (d) HSEM.

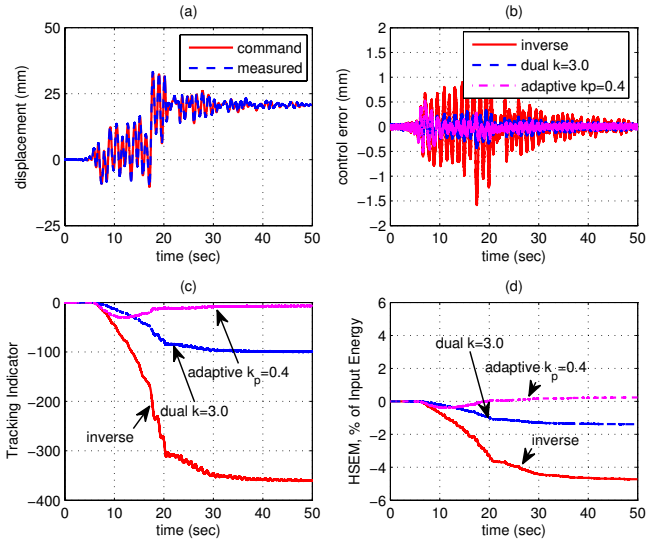

Figure 8 Real-time hybrid simulation results using compensation methods with α_{es}=45: (a) comparison of measured actuator response; (b) control error; (c) tracking indicator; (d) HSEM.

The TI values for the real-time hybrid simulation results are presented in Figs. 7(c) and 8(c). It can be observed that the TI values for the simulations with inverse compensation using poor estimates for the actuator delay (i.e., α_{es}=15 and α_{es}=45) have the largest magnitudes for the TI. For the simulations with dual compensation and adaptive compensation, the magnitudes of TI are significantly reduced, with a smaller magnitude of the TI occurring for adaptive compensation compared with that for dual compensation. Again for the cases with inverse compensation, the tracking indicator has varying slopes during the tests, indicating a variable actuator delay. The hybrid simulation energy monitor (HSEM) for the real-time hybrid simulation results is presented in Figs. 7(d) and 8(d). The values for the HSEM are shown to be around 5% and -5% for α_{es}=15 and α_{es}=45, respectively, for the cases with inverse compensation, while for the simulations with dual compensation the magnitude of the HSEM is reduced to

almost 2% and -2%, and with adaptive compensation to almost 1% and -1%. The dual compensation and the adaptive compensation methods are shown in Figs. 7 and 8 to minimize the effect of using an inaccurately estimated actuator delay in an effective manner, and the adaptive compensation scheme is shown to have the best performance.

Fig. 9 presents the history of $\Delta\alpha$ for the real-time hybrid simulations with adaptive compensation. The adaptive mechanism is shown make notable adjustments in the inverse compensation parameter beginning at around 6 sec. for the two cases when an inaccurate estimate for actuator is used.

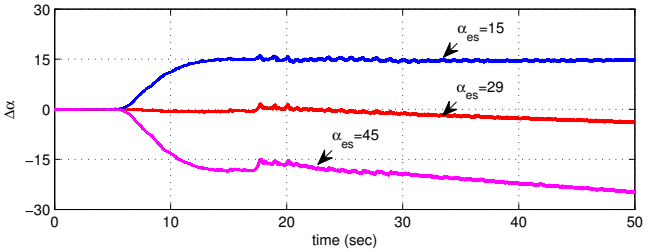

Figure 9 Time history of Δα for real-time hybrid simulations with adaptive compensation

V. SUMMARY AND CONCLUSION

An adaptive compensation method is proposed to achieve accurate actuator control in a real-time hybrid simulation. Inverse compensation with an estimated actuator delay is used. An adaptive control law is developed for the compensation parameter based on the actuator control error. The compensation parameter is adapted to minimize the error induced by an inaccurately estimated or time-varying actuator delay in a real-time hybrid simulation.

Real-time hybrid simulations of a SDOF MRF with an elastomeric damper are conducted to experimentally demonstrate the effectiveness of the proposed adaptive compensation method and to compare with two other compensation methods, including the inverse compensation and dual compensation methods. Different values of estimated actuator delay are used that include poor estimates representing an error in actuator delay by ±50% compared with the known amount of actuator delay. The tracking capability of the servo-hydraulic actuator is shown to be significantly improved and the actuator control error is greatly reduced when the adaptive compensation method is used compared with the simulation results obtained using the inverse compensation method without adaptive control. The proposed adaptive compensation scheme is shown to require minimal information about the actuator delay before the real-time hybrid simulation is performed, while enabling accurate and reliable experimental results to be achieved.

ACKNOWLEDGMENT

This paper is based upon work supported by a grant from the Pennsylvania Department of Community and Economic Development through the Pennsylvania Infrastructure Technical Alliance, and by the National Science Foundation (NSF) under Grant No. CMS-0402490 within the George E. Brown, Jr. Network for Earthquake Engineering Simulation Consortium Operation. Their support is gratefully appreciated. Any opinions, findings, and conclusions or recommendations expressed in this material are those of the authors and do not necessarily reflect the views of the sponsors.

REFERENCES

[1] T.T. Soong and B.F. Spencer Jr., "Supplemental energy dissipation: state-of-the-art and state-of-the-practice," *Engineering Structures,* vol.24, pp. 243-259, 2002.

[2] M. Nakashima, H. Kato and E. Takaoka, "Development of real-time pseudodynamic testing," *Earthquake Engineering and Structural Dynamics*, vol. 21, issue 1, pp. 79-92, 1992.

[3] T. Horiuchi, M. Inoue, T. Konno and Y. Namita, "Real-time hybrid experimental system with actuator delay compensation and its application to a piping system with energy absorber," *Earthquake Engineering and Structural Dynamics*, vol. 28, issue 10, pp.1121-1141, 1999.

[4] M.I. Wallace, J. Sieber, S.A. Neild, D.J. Wagg and B. Krauskopf, "Stability analysis of real-time dynamic substructuring using delay differential equation models," *Earthquake Engineering and Structural Dynamics*, vol. 34, issue. 15, pp. 1817-1832, 2005

[5] C. Chen and J.M. Ricles, "Stability analysis of SDOF real-time hybrid testing systems with explicit integration algorithms and actuator delay using," *Earthquake Engineering and Structural Dynamics*, vol. 37, issue 4, pp. 597-613, 2008.

[6] T. Horiuchi and T. Konno, "A new method for compensating actuator delay in real-time hybrid experiment," *Philosophical Transactions of the Royal Society of London* A, vol. 359, pp.1893-1909, 2001.

[7] R.Y. Jung and P.B. Shing, "Performance evaluation of a real-time pseudodynamic test system," *Earthquake Engineering and Structural Dynamics,* vol. 25, issue 4, pp. 333-355, 2006.

[8] C. Chen, "Development and numerical simulation of hybrid effective force testing method," PhD. Dissertation, Department of Civil and Environmental Engineering, Lehigh University, Bethlehem, PA, 2007.

[9] C. Chen and J.M. Ricles, "Improving the inverse compensation method for real-time hybrid simulation through a dual compensation scheme**,"** *Earthquake Engineering and Structural Dynamics* Published Online: DOI: 10.1002/eqe.904, 2009.

[10] A.P. Darby, A. Blakeborough and M.S. Williams, "Real-time substructure tests using hydraulic actuators," *Journal of Engineering Mechanics*, vol.125, pp. 1133-1139, 1999.

[11] P.A. Bonnet, C.N. Lim, M.S. William, A. Blakeborough, S.A. Neild, D.P. Stoten and C.A. Taylor, "Real-time hybrid experiments with newmark integration, MCSmd outer-loop control and multi-tasking strategies," *Earthquake Engineering and Structural Dynamics*, vol. 36, issue 1, pp. 119-141, 2007.

[12] K, Ogata, Discrete-Time Control Systems, 2nd Edition. Prentice-Hall, New Jersey, 1995.

[13] C. Chen, J.M. Ricles, T.M. Marullo and O. Mercan, "Real-time hybrid testing using an unconditionally stable explicit integration algorithm," *Earthquake Engineering and Structural Dynamics,* Published online, DOI: 10.1002/eqe.838, 2008.

[14] O. Mercan, "Analytical and experimental studies on large scale, real-time pseudodynamic testing," PhD. Dissertation, Department of Civil and Environmental Engineering, Lehigh University, Bethlehem, PA, 2007.

[15] Chen C, Ricles JM. Development of direct integration algorithms for structural dynamics using discrete control theory. *Journal of Engineering Mechanics*, 2008; 134(8): 676-683.

[16] Y.K. Wen, "Equivalent linearization for hysteretic systems under random excitation," *Journal of Applied Mechanics*, Transaction of ASME, vol. 47, pp.150-154, 1980.

[17] G. Mosqueda, B. Stojadinovic and S.A. Mahin, "Real-time error monitoring for hybrid simulation. Part I: methodology and experimental verification," *Journal of Structural Engineering*, vol. 133, issue 8, pp.1100-1108, 2007.